So far we have discussed the qualification of a material as a catalyst in terms of bulk properties, but the point is often made that, because catalysis is a surface phenomenon, it is the surface electronic structure that should be considered. This argument is no doubt quite valid. However, the surface electronic structure is directly related to the bulk structure and, in practice, the bulk properties seem to give good correlation with surface reactivity. An example is the phenomenon of surface film formation in corrosion, an area in which H. H. Uhlig has had considerable success in explaining a myriad of surface passivation phenomena on the basis of bulk electronic structure (*12*).

L. H. BENNETT
J. R. CUTHILL
A. J. MCALISTER
N. E. ERICKSON
Institute for Materials Research,
National Bureau of Standards,
Gaithersburg, Maryland 20760
R. E. WATSON
Brookhaven National Laboratory,
Upton, New York 11793

References and Notes

1. R. B. Levy and M. Boudart, *Science* **181**, 547 (1973).
2. D. A. Dowden and P. W. Reynolds, *Discuss. Faraday Soc.* **8**, 184 (1950); D. A. Dowden, *J. Chem. Soc. (Lond.)* (1950), p. 242; R. L. Moss and L. Whalley, *Advan. Catal.* **22**, 115 (1972); J. H. Sinfelt, J. L. Carter, D. J. C. Yates, *J. Catal.* **24**, 283 (1972).
3. R. C. Dobbyn, A. J. McAlister, J. R. Cuthill, N. E. Erickson, *Phys. Lett.*, in press.
4. J. T. Yates, Jr., and N. E. Erickson, in preparation. M. L. Perlman and J. Hudis measured the W 4*f* energy levels relative to the Au 4*f* levels (private communication).
5. L. Ramquist, K. Hamrin, G. Johansson, A. Fahlman, C. Nordling, *J. Phys. Chem. Solids* **30**, 1835 (1969); L. Ramquist, B. Ekstig, E. Kallne, E. Noreland, R. Manne, *ibid.*, p. 1849.
6. G. E. McGuire, G. K. Schweitzer, T. A. Carlson, *Inorg. Chem.* **12**, 2450 (1973).
7. F. M. Mueller, J. W. Garland, M. H. Cohen, K. H. Bennemann, *Ann. Phys. (N.Y.)* **67**, 19 (1971).
8. L. F. Mattheiss, *Phys. Rev. A* **139**, 1893 (1965).
9. An ultraviolet photoelectron spectrum for W by C. R. Feisse [*Natl. Bur. Stand. Spec. Publ. 323* (1971), p. 199] shows good agreement with the calculation by Mattheiss (*8*). Also in agreement is a calculation by I. Petroff and C. R. Viswanathan (*ibid.*, p. 53).
10. L. F. Mattheiss, *Phys. Rev.* **151**, 450 (1966).
11. A. J. McAlister, J. R. Cuthill, R. C. Dobbyn, M. L. Williams, in *Proceedings of the International Symposium on X-ray Spectra and the Electronic Structure of Matter* (Munich, 1972). A. Faessler, Ed. (in press).
12. L. H. Bennett, L. J. Swartzendruber, M. B. McNeil, in *Proceedings of the Third International Congress on Marine Corrosion and Fouling*, R. F. Acker, B. F. Rowan, J. R. DePalma, W. P. Iverson, Eds. (Northwestern Univ. Press, Evanston, Ill., 1973), p. 410.
13. We thank J. Yates for the valence band data for W and M. L. Perlman and J. Hudis of Brookhaven National Laboratory for the calibration data for W. We also thank D. Fickle for aid with sample mounting and C. Bechtoldt for x-ray diffraction measurements. R.E.W. is also a consultant with the National Bureau of Standards. Work at Brookhaven National Laboratory was supported by the Atomic Energy Commission.

27 December 1973

X-ray Photoelectron Spectroscopic Studies of Interactions in Multicomponent Metal and Metal Oxide Thin Films

Abstract. *Changes in chemical oxidation states in alloys and at solid-solid interfaces were monitored by using x-ray photoelectron spectroscopy. For an oxidized Nichrome surface, the chromium component was selectively converted to chromic oxide while nickel remained in the metallic state. When this surface was overlaid with a 20-angstrom-thick aluminum film, the chromic oxide was reduced to chromium and the aluminum was oxidized to aluminum oxide in a reaction zone consisting of no more than 10 angstroms of the interface. This scheme appeared general for solid-solid contacts and was predicted, to a first approximation, by bulk thermodynamic free energies.*

Much of the research on the structure and chemical composition of thin film surfaces during the last several decades was restricted to relatively thick layers because of the sample requirements of the available analytical techniques (*1*). Recently, however, there has been an expansive development of a variety of new spectroscopic methods, such as electron diffraction, Auger spectroscopy, secondary ion mass spectroscopy, ion scattering spectrometry, and microprobe methods, which are capable of characterizing structure and composition for material present in only fractional monolayers. Of particular interest is x-ray photoelectron spectroscopy (XPS); in addition to providing elemental analyses, this technique measures the electron binding energy, and chemical shifts of this energy are often directly relatable to molecular structure and bonding.

Considerable emphasis is currently being placed on characterizing the surface structure of multicomponent substrates, which are attractive as new materials in catalysis, corrosion inhibition, and electrochemistry. For example, Auger spectroscopic studies indicate differences between surface and bulk concentrations in alloys (*2*). Further changes have been noted after an alloy surface is exposed to oxygen, due to the preference of oxygen for one of the alloy components (*3*). Ion microprobe studies of Fe_2O_3 doped with Al have examined the passivating effect this treatment has on Fe_2O_3 substrates, and excess surface concentrations of Al have been noted (*4*). Several low-energy electron diffraction studies have elucidated the types of surface interactions that are involved in these multicomponent systems. For example, it has been suggested (*5*) that Cs and O absorbed on the (100) or (112) planes of W form a Cs-O-W double layer regardless of which species was deposited first.

Perhaps the best chemical information on these systems can be obtained by XPS techniques, although there are few examples from the literature to support this claim. The oxidation of a NiCu

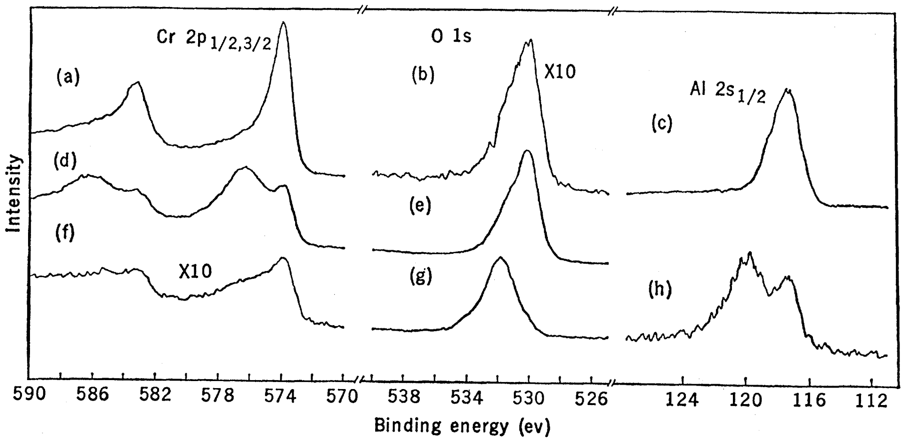

Fig. 1. X-ray photoelectron spectra. (a) Chromium chip evaporated at 1×10^{-7} torr onto Cu foil. (b) Residual oxygen from the sample in (a). (c) Aluminum wire evaporated at 1×10^{-7} torr onto Cu foil. (d) and (e) Oxidized Cr surface from (a) after exposure to 0.01 atm of oxygen for 30 seconds. An identical spectrum is obtained for the Cr component in an oxidized Nichrome film. (f), (g), and (h) Chromium surface (d) overlaid with about 20 Å of Al. Note the relative decrease in oxide shoulder on the Cr $2p_{1/2,3/2}$ peaks and the shift of the O 1*s* peak to 532.0 ev, now characteristic of Al_2O_3.

alloy (70 percent Ni, 30 percent Cu) has been studied by this method and both CuO and NiO have been identified as surface species (*6, 7*). The possibility that metallic Cu was present in the NiO lattice was proposed but never confirmed.

We have studied the system Ni, Cr, O, and Al with the objective of monitoring the chemical changes that occur when the various components are mixed. This system is important in the microelectronics industry since Al is commonly used as the conducting contact with Nichrome thin film resistors. Our XPS data for Nichrome exposed to oxygen show that Cr is preferentially oxidized and Ni remains in the metallic state. In addition, when the Nichrome surface is coated with a thin film of Al, the interfacial oxygen is no longer bonded to the Nichrome substrate, but forms a thin Al_2O_3 layer. In the first-order approximation, these reactions are well predicted by the bulk thermodynamic free energies.

Spectra were obtained on a Hewlett-Packard model 5950A x-ray photoelectron spectrometer; the sample system has been described elsewhere (*8*). All binding energies are reported with respect to the $4f_{7/2}$ line of Au at 84.0 ev. Oxygen (Matheson, research grade) could be introduced into a sample treatment chamber on the spectrometer via a gas manifold and variable leak valve. Pressures in this chamber, as measured by a nude Bayard-Alpert gauge, were around 1×10^{-8} torr, although during evaporations the treatment chamber pressure would rise to 1×10^{-7} torr. The spectra of evaporated Cr, Al, and Ni are shown in Fig. 1a, Fig. 1c, and Fig. 2a, respectively. The wide-scan spectra for these metals showed no significant impurity, except for the O 1*s* signal with an intensity characteristic of an amount of oxygen equivalent to a fraction of a monolayer. The surfaces are stable in the spectrometer at 10^{-8} torr for up to an hour, with only a slight increase in the O 1*s* signal and the appearance of a trace N 1*s* signal from the Cr sample.

Bimetallic samples can be prepared, for example by evaporating a thin film of Al onto the Cr substrate. The photoelectron intensity from the substrate decreases exponentially with the thickness of the overlay (*9*)

$$I = I^{\circ} e^{-1.61\, d/\lambda} \qquad (1)$$

where λ is the mean escape depth for inelastic collision of the electrons in the overlay, I° is the initial number of counts detected from the Cr sample, *I* is the number of counts obtained from Cr after the evaporation, and *d* is the thickness of the Al overlay. We chose $\lambda = 15$ Å as a typical value for this system (*9*). The factor 1.61 arises from the angle between the sample surface and the entrance aperture of the spectrometer. Deposition of 20 Å of Al over Cr (as indicated by a tenfold decrease in the Cr signal) does not produce a shift in binding energy for either species, indicating no observable interactions between the two layers. In addition, in this case, heating the sample to 300°C does not change the intensity ratio of the Cr and Al signals, indicating no interdiffusion or islanding of the evaporated film as the temperature is increased.

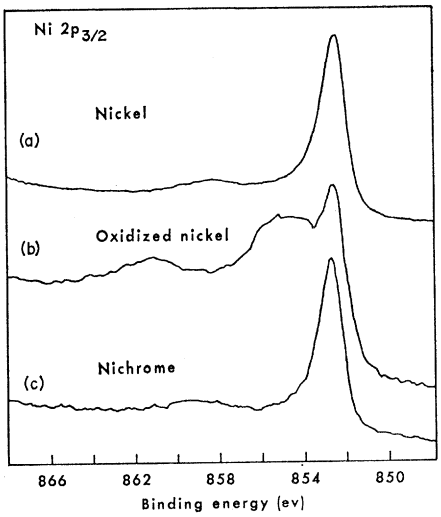

Fig. 2. Nickel $2p_{3/2}$ XPS spectra of (a) Ni wire evaporated at 1×10^{-7} torr onto Cu foil, (b) the surface from (a) exposed to 0.01 atm of oxygen for 30 seconds, and (c) Nichrome evaporated at 1×10^{-7} torr onto Cu foil (exposure of this sample to 0.01 atm of oxygen for 30 seconds reduced the intensity slightly but did not affect the spectral shape).

Similar results are not observed when oxygen first reacts with the Cr surface. As shown in Fig. 1d, a "clean" Cr surface forms an oxide layer several angstroms thick when exposed to 0.01 atm of dry oxygen. The presence of two O 1*s* peaks at 530.1 and 531.3 ev in Fig. 1e is surprising since during the initial oxidation only one oxide, Cr_2O_3, is expected (*10*). From our previous experience, however, different crystal structures (*11*) or unusual oxidation states (*12*) stabilized on the surface are often found. This O 1*s* doublet may well be understood in terms of either of these phenomena. Evaporation of a 20-Å layer of Al onto this substrate causes a drastic alteration in the chemistry. The oxygen initially associated with the Cr as Cr_2O_3 is now associated with Al, probably as Al_2O_3 (*13*). This is verified by (i) the decrease in the oxide shoulder on Cr (Fig. 1, d and f); (ii) the increase in the oxide shoulder on Al (Fig. 1, c and h) and (iii) the shift in the O 1*s* peak from a "Cr_2O_3-like" value to an "Al_2O_3-like" value (Fig. 1, e and g). From the relative amounts of the decrease in the oxide shoulder on Cr, the reaction zone appears no greater than 10 Å. The spectra remain virtually unchanged when the samples are heated to 300°C. Thus, we conclude that within two or three layers at the interface the reaction

$$Cr_2O_3 + 2Al \rightarrow 2Cr + Al_2O_3 \qquad (2)$$

will predominate.

The driving force, ΔG, based on thermodynamic values for the bulk species, is -127 kcal/mole and is highly favorable for this reaction. Its occurrence might well be expected at an interface if the local contributions to the energy are not sufficient to override the available chemical free energy. We have tested this idea with other systems. For example, our group (*11, 12*) as well as other workers (*14*) have found that gold can be evaporated on most metal oxides without any interfacial reactions of the type in reaction 2. This is understandable since Au_2O_3 has a positive free energy of formation. However, evaporation of Pb onto Au_2O_3 produces immediate interfacial formation of Au and PbO, a reaction with $\Delta G = -175$ kcal/mole.

Similar selective oxidation of multicomponent systems is also observed in alloys. Evaporation of NiCr wire with 80 percent Ni and 20 percent Cr produces a layer whose surface concentration is 65 percent Ni and 35 percent Cr, as determined by comparing the photoelectron count rates to those of pure Ni and Cr. Exposure of this surface to 0.01 atm of oxygen at temperatures from 25° to 300°C produces Cr_2O_3, as indicated by the O 1*s* and Cr $2p_{3/2}$ binding energy values (Fig. 1, d and e). The Ni species is not oxidized; as shown in Fig. 2c, the spectrum remains virtually identical to that of a clean Ni surface (Fig. 2a). In addition, the surface concentration of the oxidized alloy changes to 50 percent Ni and 50 percent Cr, where the Cr concentration includes all visible metallic Cr and Cr_2O_3. Note that exposure of pure Ni to 0.01 atm of oxygen (Fig. 2b) results in several layers of NiO and Ni_2O_3 (*13*), whereas Ni in the Cr matrix does not oxidize. This selective oxidation is also seen on Nichrome films which have been treated in air at 400°C for several minutes. Evaporation of a thin Al overlay on this oxidized Nichrome sample again results in reduction of the Cr_2O_3 component to Cr and oxidation of Al to Al_2O_3 as in reaction 2.

It is clear that under these experimental conditions Cr completely prevents oxidation of Ni. This observation is certainly counter to the prediction that the high surface electric fields prevent such selective oxidation schemes (*7*). The fact that oxygen has a higher affinity for Cr than for Ni apparently is the major factor in determining the reaction products and is responsible for the increased total surface concentration of Cr.

We know of no other analytical method that has the combination of depth resolution, sensitivity to elements and oxidation states, and low probing energy required to make these measurements. These results will be useful in a number of disciplines. In microelectronics, we postulate (*15*) an explanation for the failure mechanism of Nichrome resistors. These resistors, made by thin film deposition of Nichrome followed by an oxidizing treatment to adjust to the desired resistance, have Al contacts and conductors. Reaction 2 results in a high-resistance contact due to the presence of an Al_2O_3 interfacial film. We also expect bonding of one material to another, especially metals to oxides or oxidized surfaces, to involve this type of reaction. In addition, in catalysis this scheme may be relevant for understanding experimental observations involving the poisoning of catalytic surfaces, the dispersion of supported metals, and the behavior of metallic clusters.

NICHOLAS WINOGRAD
W. E. BAITINGER, J. W. AMY
Department of Chemistry,
Purdue University,
West Lafayette, Indiana 47907
J. A. MUNARIN
Strategic Systems and Components
Division, Naval Ammunition Depot,
Crane, Indiana 47522

References and Notes

1. D. F. Klemperer, in *Chemisorption and Reactions on Metallic Films*, J. R. Anderson, Ed. (Academic Press, New York, 1971), pp. 40–117.
2. H. Shimizer, M. Ono, K. Nakayama, *Surface Sci.* **36**, 817 (1973).
3. F. Williams and M. Boudart, *J. Catal.* **30**, 393 (1973).
4. J. Von Fraunhofer, T. Hoar, G. Pickup, *Nat. Phys. Sci.* **229**, 88 (1971).
5. C. Papageorgopoulos and J. M. Chen, *Surface Sci.* **39**, 313 (1973).
6. L. D. Hulett, A. L. Bacarella, L. LiDonnici, J. C. Griess, *J. Electron Spectrosc.* **1**, 169 (1972/73).
7. J. E. Castle, *Nat. Phys. Sci.* **234**, 93 (1971).
8. K. Siegbahn, D. Hammond, H. Fellner-Feldegg, E. F. Barnett, *Science* **176**, 245 (1972).
9. W. A. Fraser, J. V. Florid, W. N. Delgass, W. D. Robertson, *Surface Sci.* **36**, 661 (1973); T. A. Carlson and G. E. McGuire, *J. Electron Spectrosc.* **1**, 161 (1972/73).
10. P. Michel and C. H. Jardin, *Surface Sci.* **36**, 478 (1973).
11. K. S. Kim and N. Winograd, *Chem. Phys. Lett.* **19**, 209 (1973); K. S. Kim, T. J. O'Leary, N. Winograd, *Anal. Chem.* **45**, 2214 (1973).
12. K. S. Kim and N. Winograd, *Surface Sci.*, in press.
13. A. Barrie, *Chem. Phys. Lett.* **19**, 109 (1973).
14. W. P. Davis and J. E. Lester, *Anal. Chem.* **45**, 1416 (1973).
15. W. E. Baitinger, N. Winograd, J. W. Amy, J. Munarin, in preparation.
16. Supported by National Science Foundation grants GP-37017X and GH-335741A1, and by Air Force Office of Scientific Research grant AFOSR-72-2238. We also thank Kwang S. Kim for his many helpful discussions.

10 December 1973; revised 30 January 1974 ■

Cristobalitic Stage in the Diagenesis of Diatomaceous Shale

Abstract. *With increasing depth of burial, diagenetic cristobalite in the Monterey Shale of California shows a decrease in the* d(*101*) *spacing from 4.115 to 4.040 angstroms, indicative of a progressive change in its internal structure. The spacing is 0.004 to 0.015 angstrom smaller in porcellanite than in associated chert, probably because the cristobalite of porcellanite formed later than that of chert.*

Interest in diagenetic alteration of biogenic opal into chert has revived in recent years, largely because of the discovery of much chert in deep-sea sediments and the trouble caused by the chert in the drilling of these sediments. The experience of the Deep Sea Drilling Project has been described in many reports, of which only a few can be cited here (*1, 2*).

We have sampled thick sections of the Miocene Monterey Shale of California in the course of a geochemical study of Tertiary sedimentary rocks (*3*). Bramlette (*4*, pp. 16–17) recognized that metamorphism due to burial converted diatomaceous Monterey Shale first into "opaline" cristobalitic chert and porcellanite and finally into quartzitic chert and porcellanite. The use of x-ray techniques has allowed us to study these conversions in greater detail.

The main stages of diagenesis and the rock terms used by us are explained by reference to a typical exposure of Monterey Shale (Fig. 1). Rocks in the exposure are alternating layers of dark compact chert and light porous porcellanite, which are distinguished in the field on the basis of texture (*2, 4*) and whose mineralogy is determined in the laboratory through x-ray diffraction. Both chert and porcellanite of this exposure yield diffraction patterns of low cristobalite.

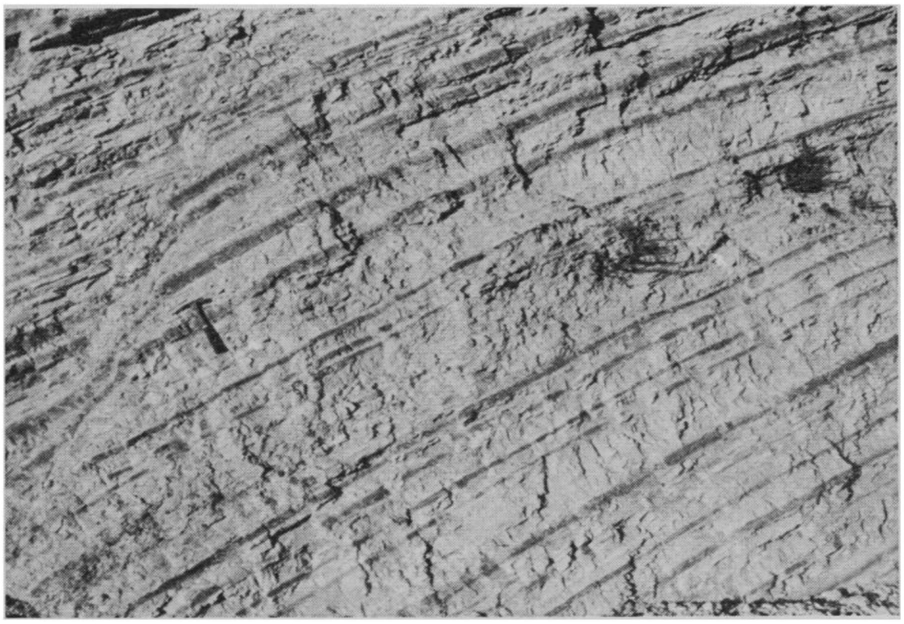

Fig. 1. Exposure of Monterey Shale along Sweeney Road east of Lompoc, California, consisting of thin dark beds of cristobalitic chert alternating with thicker light-colored beds of cristobalitic porcellanite. The hammer is 33 cm long.